Fast Millimeter Wave Threat Detection Algorithm

I. Gómez Maqueda[1], N. Pérez de la Blanca[1], R. Molina[1], A.K. Katsaggelos[2]

[1] Dept. of Computer Science and Artificial Intelligence, University of Granada, Granada, Spain.
[2] Dept. of Electrical Engineering and Computer Science, Northwestern University, Evanston, USA
{igomezmaqueda,nicolas,rms}@decsai.ugr.es, aggk@eecs.northwestern.edu

ABSTRACT

Millimeter Wave (MMW) imaging systems are currently being used to detect hidden threats. Unfortunately the current performance of detection algorithms is very poor due to the presence of severe noise, the low resolution of MMW images and, in general, the poor quality of the acquired images. In this paper we present a new real time MMW threat detection algorithm based on a tailored denoising, body and threat segmentation, and threat detection process that outperforms currently existing detection procedures. A complete comparison with a state of art threat detection algorithm is presented in the experimental section.

Index Terms—Millimeter wave imaging, image processing , Security.

1. INTRODUCTION

Passive Millimeter Wave (PMMW) imaging occurs through the detection of radiometric temperature differences of the various objects in the scene. Unfortunately, due to their characteristics, the quality of the acquired PMMW images is very poor, see Figure 1.

MMW images can be used to detect weapons or contraband concealed on subjects both in active and passive systems [1], [2]. They are been increasingly used in security applications to protect the security of public areas and services like trains and underground stations, airports, government buildings, military facilities, and checkpoints.

The increasing interest in security and surveillance has fostered the research and development of this kind of systems, e.g. the design of new detectors [3], [4] to obtain receiver modules [5]-[6] for passive imaging systems [7]-[9], the development of a variety of active imaging systems in MMW-band [10] and THz-band [11]-[12], and the new advances in radar systems in THz-band [13]-[14].

Unfortunately, since very frequently automatic detection algorithms produce very high false alarm rates, threats in the images must be detected by an operator. However, it has been estimated that the maximum operator screening rate is 120-140 person/hour while the Transportation Security Administration (TSA) aims at a processing speeds of 240 passengers per hour.

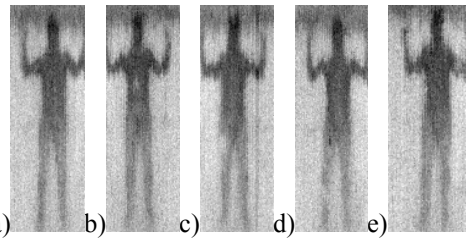

a) Subject without threat; b) Subject carrying 175 ml of alcohol in his chest; c) Person carrying a CD in his trousers' pocket; d) Person carrying plasticine in his shin; e) Subject carrying metallic bags.

Fig. 1. MWW sample images.

Passive MMW images have inherits limitations which make the detection of hidden threats a hard problem:

- Low resolution images: image typically of size 200x60 pixels.
- High pixel size: each pixel has a size of about several millimeters due to working wavelength.
- Passive radiometry implies very low Signal to Noise ratio (SNR). It is important to note that the amount of radiation emitted in the millimeter-wave range is 10^8 times smaller than the amount emitted in the infrared range. Some commercial MMW systems have a thermal sensitivity up to 5ºK which precludes their use.
- Intensity inhomogeneity due to temperature differences in the scene.
- Limitations of the current acquisition systems.

An approach to mitigate some of these limitations is to increase operating frequency. An increase in the working frequency translates into higher resolution images. However, given the electronic's state of the art, signal to noise ratio can be worse.

Previous works have addressed the automatic threat detection problem on MMW images. In [15], two segmentation methods are presented: K-means and Active Shape Models (ASM). K-means is applied over the intensity histogram to classify the background, the body and threats. Results show unconnected classifications and the need to introduce heuristics in order to determine the number of clusters. Classification is then done by per-

This paper has been supported by the Spanish Ministry of Economy and Competitiveness under project TIN2013-43880-R, the European Regional Development Fund (FEDER), and the Department of Energy (DE-NA0002520).

forming maximum-likelihood estimation with the pre-computed Probability Density Functions (PDFs) of background and foreground. To improve the connectivity of the segmented body an ASM is used over the results obtained using k-means. However, modelling the full range positions of the body with an ASM is a very complex task [15].

In [16], which is an extension of [15], weighted mixture models are estimated depending on the scenario. To classify objects, the Expectation Maximization (EM) algorithm is applied. Results show an improvement on the accuracy of the segmentation but still the method has problems with unconnected segmentation.

In [7], a two stage algorithm is applied. Firstly, an Iterative Steering Kernel Regression (ISKR) or a Non Local Means denoising algorithms are applied to MMW images. Secondly, a Local Binary Fitting (LBF) algorithm is utilized to separate background, body and threats. Results show that the combination of ISKR and LBF algorithms obtains accuracy values around 90%. However, ISKR and LBF algorithms are time consuming algorithms that cannot be used in real time applications.

In this paper, we focus on the design of a real time algorithm to detect threats in MMW images. Similarly to [7] we propose an algorithm based on two phases: denoising and classification. In order to make our algorithm applicable in real time we propose a convenient combination of denoising filters to locate the possible threats on the image and the use a very simple but effective classification rule. The paper is organized as follows. In section 2 we present the complete threat detection algorithm. Section 3 contains the validation of the proposed approach and section 4 concludes the paper.

2. THREAT DETECTION ALGORITHM

The complete threat detection algorithm consists of three major steps: a) MMW receiver modeling, which aims at modeling and removal the image noise; b) body & threat region segmentation from background, and; c) threat detection. We now describe the three steps in details.

MMW Receiver modeling and denoising. Given the MMW image quality, the first step of the threat detection algorithm must be the modelling and removal of the image noise and improving the contrast between regions. We start by modeling the background emission. To achieve this goal we estimate the mean and standard deviation pixel maps. These maps are obtained by averaging 9 background images to estimate each pixel's response and smoothing the maps with a 2D Gaussian filter to reduce spatial noise. Figure 2 shows the computed mean and standard deviation maps. Figure 2a) shows 3 background MMW image samples. The top black bars correspond to heated objects, which are used for calibration. The images present a deformation pattern across the image columns due to the vertical scanning pattern. In the horizontal direction the behavior is stable. Figure 2b) shows the estimated mean map. Comparing the map in Figure 2b) with the images in Figure 1a), it can be concluded that the estimated map matches very well the background pattern. Figure 2c) shows the standard deviation map. It shows a rather uniform behavior across the image.

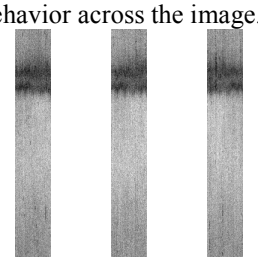

(a) Background MMW images samples.

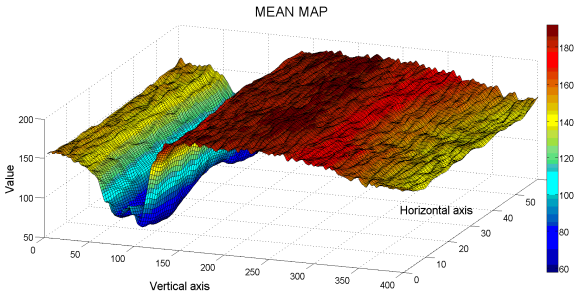

(b) Mean map

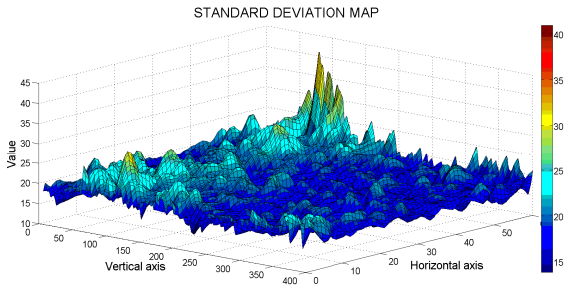

(c) Standard deviation map

Fig. 2. Mean and standard deviation maps

To remove the image noise a severe smoothing step is applied. Firstly, in order to remove noise without smoothing the image borders we apply to the raw image a fixed 5x5 median filter, then a 3x3 Gaussian filter with standard deviation 1. Then, we compare pixel by pixel the smoothed image with the estimated background mean map. Those image pixels with values in an interval centered in the corresponding mean map value are mapped to the mean map value. With this step we separate the background from a region defined by body plus threat. Inside the body plus threat region some noise still remains. To reduce it we perform smoothing again using a new combination of non-linear (median) filter and a linear filter (Gaussian convolution). Finally, we enhance image edges to facilitate the body plus threat segmentation step. In Figure 3a) two original images (1st and 3rd from left to right) and their corresponding processed images (2nd and 4th) are shown. The processed images form the input to the next algorithmic step.

Body & threat segmentation. Body pixel values are clearly separated from background values, but threat regions are nearer to background values. Therefore, two different segmentations are carried out to obtain the body and a first threat masks. A binary segmentation algorithm based on Otsu's thresholding algorithm [17] is used to

obtain the body mask. Figure 3b) shows the result of applying Otsu's algorithm to the second and fourth images in Figure 3a). Although the body is adequately segmented, some threat regions are eliminated.

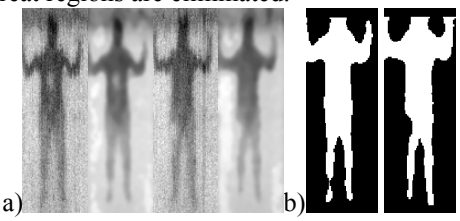

Fig. 3. a) Original and preprocessed MMW image pairs; b) Otsu segmented images from the second and fourth images on the left.

A threat can be defined as a small local region of different emissivity inside or near the body outline. Then we estimate the threat binary mask applying a standard adaptive thresholding algorithm using an average kernel size of 21 x 21 pixels on the smoothed image. That is, on each pixel the average value $p_{i,j}$ of the image intensities $f_{i,j}$ in a 21x21 window centered at pixel i,j is computed,

$$p_{i,j} = \frac{1}{121}\sum_{k=-10}^{10}\sum_{l=-10}^{10} f_{i+k,j+l} \quad (1)$$

The obtained value is compared with the original one to produce a binary mask.

$$g_{i,j} = \begin{cases} 1 & if\ (p_{i,j} - f_{i,j}) > 0 \\ 0 & if\ (p_{i,j} - f_{i,j}) < 0 \end{cases} \quad (2)$$

The fourth column of figure 4 shows several examples of the output of this step. A pixel (i,j) with $g_{i,j}$=1 is a potential detected threat; however, it must be in contact with (or very close to) the body segmentation provided by Otsu's method. This is analyzed in the next algorithmic step.

Threat detection. Since threats are assumed to be inside or in contact with the body, we examine the 1-labeled connected regions in g which are at most at distance two from the body segmentation provided by Otsu methods and mark them as threats.

3. EXPERIMENTAL RESULTS

In this section we compare our approach to the method proposed in [7]. This paper utilizes a two stage algorithm based on Iterative Steering Kernel Regression (ISKR) and Local Binary Fitting (LBF). The ISKR algorithm removes the noise in the MMW image and the LBF algorithm tries to find hidden threats.

The database we used is composed by 36 MMW images with threats hidden across the body (chest, thigh, shin, and arm). Figure 1 shows a sample of our MMW image database. Threats are Improvised Explosive Devices (IED's) with both metallic and dielectric threats. The threats used are: 1) CD in a plastic bag; 2) 175 ml of Alcohol; 3) A pack of 9x7x1 cm of plasticine (150g); 4) Scissors; 5) Metallic pieces in a bag (size: 9x6x1 cm); 6) 100 grams of Calcium sulphate (10x6 cm); 7) Metallic bags 8x12x1; 8) 200 ml of room temperature water. The database also contains subject images without hidden threats. A sample is shown in Fig.1

Table 1 shows the accuracy (Acc_1) and False Positive (FP_1) rates obtained using the ISKR+LBF algorithms. Notice that these rates are computed by comparing, through visual inspection, the output of the algorithm with the ground truth and declaring success if the real and detected threats coincide in their locations. Results show poor accuracy results and a high false positive rate. The differences between these results and the figures shown in [7] are due to the use of smaller threats and harder locations. In [7] the average threat size was around 500 grams and 20x20x5 cm^3 while in our database threats have an average size of about 150 grams and a size of 10x10x1 cm^3.

Experiment	Acc_1	FP_1
Chest	50%	10%
Thigh	0%	20%
Shin	0%	20%
Arm	12.5%	30%

Table 1. Accuracy and false positives rates with ISKR+LBF algorithms.

Figure 4 shows, row-wise, the output of each one of the stages of the proposed algorithm working on three images where the threats are inside and in the outline of the body. To denoise the image, Gaussian filters of size 3x3 and standard deviation equal to 1.5 are applied, while 5x5 filters are used for median filtering. The width of the interval to map the mean background values on the image was fixed to [1.0 1.5] standard deviations on each pixel. All the experimental parameters were fixed by empirical evaluation.

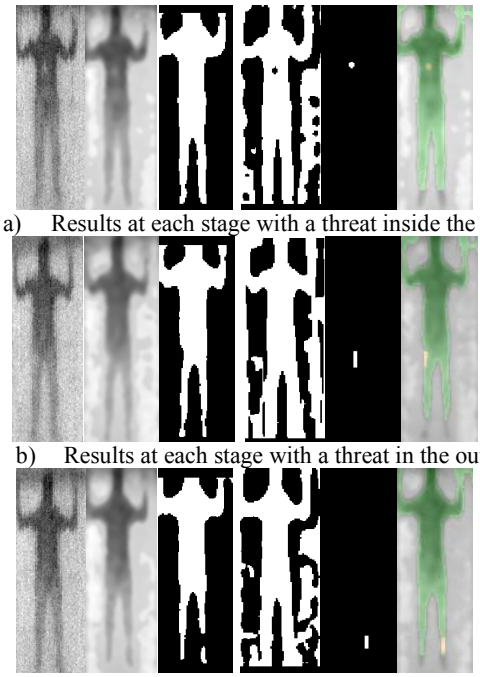

a) Results at each stage with a threat inside the body.

b) Results at each stage with a threat in the outline

c) Results at each stage with a threat in the outline (shin)

Fig. 4. Experimental comparison. From left to right, raw image, filtered image, body segmented image, thread detection, estimated thread location and fused images.

Table 2 shows the detection result obtained. Comparing with Table 1, it is concluded that the accuracy of the proposed algorithm is significantly better in all threat

locations without increasing the false positive rate. Average accuracy rises from 15.5% to 56.75%.

Experiment	Acc_2	FP_2
Chest	88.9%	10%
Thigh	50%	10%
Shin	62.5%	20%
Arm	25%	20%

Table 2. Accuracy and false positives rates with of our proposed algorithm.

Figure 5 shows a comparison of both algorithms on relevant database samples. In the first two images a threat is located at the human chest. Both algorithms detect the threats (ISKR+LBF shows good results on the chest). In images 3 and 4 threats are in the human thigh, in images 4 and 5 threats are in the human shin and in image 7 the threat is in the arm. In these images ISKR+LBF does not detect any threat while our approach detects all of them (see red spots in the images). A higher performance of our algorithm over the ISKR+LBF combination can be concluded.

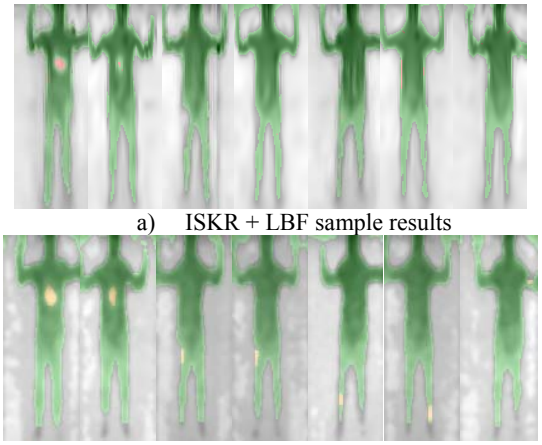

a) ISKR + LBF sample results

b) Sample results obtained by our algorithm

Fig. 5. Experimental comparison.

Table 3 shows the processing time for both algorithms on an Intel Core i7-4700MQ 2.4GHz with a RAM of 8GB.

Algorithm	Proposed in [7]	Our proposed algorithm
Denoising	37200 ms	12 ms
Body segmentation	439 ms	5 ms
Threat detection		3 ms
Total	**37639 ms**	**20 ms**

Table 3. Comparison of processing times.

Figure 6 shows the ROC curve for both algorithms compared. Notice how the proposed algorithm outperforms the one in [7].

Figure 7 shows additional sample results of the comparison of both algorithms. These images show wrong results from both algorithms. The first row, fig7 a), shows the raw images. From left to right, the threat on each image is: {threat number 6 in his chest, no threat, threat 2 in his thigh, threat number 3 in his shin, threats 4 in his arm, threats 4 in his arm}. In the second row, fig7 b), the result of applying the ISKR+LBF algorithm is shown. This algorithm report false positives in images 1, 3, 5, 6 and 7 with a total of 7 false positives; and does not detect any of the threats. Besides the wrong results, it is important to note the incorrect segmentation of the person in many of these images (see images fifth to seventh in figure 7a). In the third row, fig7 c), the results of our algorithm is shown. The proposed developed algorithm also does not detect any of the 5 threats carried and reports 4 false positive results. These wrong results in our case are mainly due to the need of fixing the filter parameter on each image according to its noise level. Some of these wrong results can be solved adapting the filter parameters which point out on the interest of adapting the proposed algorithm to estimate the free parameters on each image.

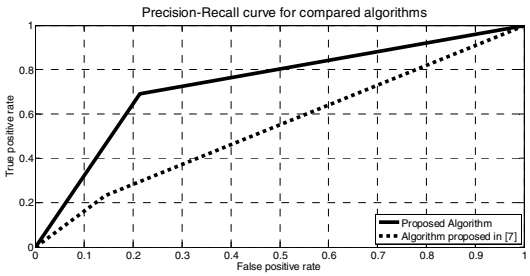

Fig. 6. ROC curve.

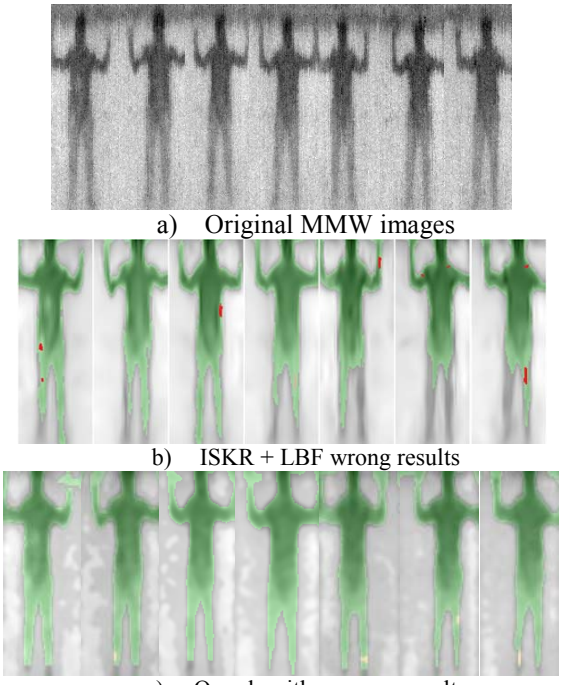

a) Original MMW images

b) ISKR + LBF wrong results

c) Our algorithm wrong results

Fig. 7. Wrong sample results from both algorithms.

5. CONCLUSIONS

A new method for filtering and threat detection on MMW images has been proposed and a comparative study with a state of the art technique on a new database of 36 MMW images has been carried out. The reported results show that our algorithm for detecting threats clearly outperforms current methods in terms of accuracy and false

positive rate. The average improvement on the state of the art technique is higher than 40%. Furthermore, our algorithm reduces the false alarm rate by 5%, placing the mean value of the false alarm rate as low as 15%. The developed algorithm reduces the processing time by a 2000 factor, making it usable in real time operation modes.

In spite of the promising results, more research has to be carried out in order to increase accuracy rates in areas like arms and legs where threats are sometimes not detected. For these cases different improvements based on a multilevel segmentation algorithm [19], analysis of the body outline and free parameter estimation must be considered. Also fusion with information from other image cues, such as depth, will potentially improve the detection of hidden threats and will be explored in the future.

REFERENCES

[1] N. E. Alexander, C. Callejero and R. Gonzalo, "Multispectral mm-wave imaging: materials and images", Proc. SPIE 6948, 2008.

[2] R. Appleby and H.B. Wallace, "Standoff Detection or Weapons and Contraband in the 100 GHz to 1 THz region", IEEE Trans. Antennas Propagat., vol.55, Nov. 2007.

[3] H.P. Moyer, J.N. Schulman, J.J. Lynch, J.H. Schaffner, M. Sokolich, Y. Royter, R.L. Bowen, C.F. McGuire, M. Hu and A. Schmitz, "W-Band Sb-Diode Detector MMICs for Passive Millimeter Wave Imaging," IEEE Microw. Compon. Lett., vol.18, no.10, pp.686-688, Oct. 2008.

[4] J.W. May and G.M. Rebeiz, "Design and Characterization of W-Band SiGe RFICs for Passive Millimeter-Wave Imaging," IEEE Trans. Microw. Theory Techn., vol.58, no.5, pp.1420-1430, May 2010.

[5] J.J. Lynch, H.P. Moyer, J.H. Schaffner, Y. Royter, M. Sokolich, B. Hughes, Y.J. Yoon and J.N. Schulman, "Passive Millimeter-Wave Imaging Module With Preamplified Zero-Bias Detection," IEEE Trans. Microw. Theory Techn, vol.56, no.7, pp.1592- 1600, July 2008.

[6] L. Gilreath, V. Jain, H.-C. Yao, L. Zheng and P. Heydari, "A 94- GHz passive imaging receiver using a balanced LNA with embedded Dicke switch," IEEE Radio Frequency Integrated Circuits Symposium, vol.,pp.79-82, May 2010.

[7] O. Martínez, L. Ferraz, X. Binefa, I. Gómez, and C. Dorronsoro, "Concealed object detection and segmentation over millimetric waves images," IEEE Computer Society Conference on Computer Vision and Pattern Recognition Workshops (CVPRW), pp.31-37, 13-18 June 2010.

[8] K. Yamada, K. Morichika, T. Hasegawa, H. Hirai, H. Niikura, T. Matsuzaki and J. Nakada, "Development of 77 GHz millimeter wave passive imaging camera," IEEE Sensors J., pp.1632-1635, 25-28 Oct. 2009.

[9] K. K. Jung, S. W. Yoon, Y. S. Chae and J. K. Rhee, "Development of a passive millimeter-wave imaging system," Waveform Diversity and Design Conference, Feb. 2009.

[10] D.M. Sheen, D.L. McMakin, T.E. Hall and R.H. Severtsen, "Active millimeter-wave standoff and portal imaging techniques for personnel screening," IEEE Conference on Technologies for Homeland Security, pp.440-447, 11-12 May 2009.

[11] V. Krozer, T. Lo ffler, J. Dall, A. Kusk, F. Eichhorn, R.K. Olsson, J.D. Buron, P.U. Jepsen, V. Zhurbenko,and T. Jensen, "Terahertz Imaging Systems With Aperture Synthesis Techniques," IEEE Trans. Microw. Theory Techn., vol.58, no.7, pp.2027-2039, July 2010.

[12] F. Friederich, W. von Spiegel, M. Bauer, F. Meng, M.D. Thomson, S. Boppel, A. Lisauskas, B. Hils, V. Krozer, A. Keil, T. Loffler, R. Henneberger, A.K. Huhn, G. Spickermann, P.H. Bolivar and H.G. Roskos, "THz Active Imaging Systems With Real-Time Capabilities," IEEE Trans. Terahertz Science and Technology, vol.1, no.1, pp.183-200, Sept. 2011.

[13] K.B. Cooper, R.J. Dengler, N. Llombart, B. Thomas, G. Chattopadhyay and P.H. Siegel, "THz Imaging Radar for Standoff Personnel Screening," IEEE Trans. Terahertz Science and Technology, vol.1, no.1, pp.169-182, Sept. 2011.

[14] N. Lombart, K.B. Cooper, R.J. Dengler, T.Bryllert and P.H. Siegel, "Confocal Ellipsoidal Reflector System for a Mechanically Scanned Active Terahertz Imager", IEEE Trans. Antennas Propagat., vol. 58, no. 6, pp 1834-1841, June 2010.

[15] C. Haworth, B. Gonzalez, M. Tomsin, R. Appleby, P. Coward, A. Harvey, K. Lebart, Y. Petillot, and E. Trucco. Image analysis for object detection in millimetre-wave images. In R. Appleby, J. Chamberlain, and K. Krapels, editors, Conference on Passive Millimetre-Wave and Terahertz Imaging and Technology, volume 5619 of SPIE, pages 117–128, 2004.

[16] C. D. Haworth, Y. R. Petillot, and E. Trucco. "Image processing techniques for metallic object detection with millimetre wave images". Pattern Recognition Letters, 27(15):1843– 1851, 2006.

[17] Nobuyuki Otsu "A threshold selection method from gray-level histograms". IEEE Trans. Sys., Man., Cyber. 1979.

[18] Comaniciu, D.; Meer, P., "Mean shift: a robust approach toward feature space analysis," Pattern Analysis and Machine Intelligence, IEEE Transactions on , vol.24, no.5, pp.603,619, May 2002

[19] M. Luessi, M. Eichmann, G. M. Schuster, and A. K. Katsaggelos, "A Framework for Efficient Multilevel Image Thresholding," Journal of Electronic Imaging, vol. 18, issue 1: SPIE, Jan. 2009.

[20] N. Gopalsami, S. Liao, T. W. Elmer, E. R. Koehl, A. Heifetz, A. C. Raptis, L. Spinoulas, and A. K. Katsaggelos, "Passive Millimeter Wave Imaging with Compressive Sensing," Optical Engineering, Special Issue on Terahertz and Millimeter Wave Imaging, vol. 51, no. 9, pp. 091614-1:091614-9, Sept. 2012.